Investigation of the Radiative Power Loss in the Limiter Plasmas of W7-X

D. Zhang[1], R. Burhenn[1], B. Buttenschön[1], R. König[1], R. Laube[1], H. Jenszch[1], L. Giannone[2], M. Marquardt[1], H. Thomsen[1], A. Werner[1], A. Alonso[4], Ch. Biedermann[1], S. Bozhenkov[1], R. Brakel[1], A. Czarnecka[6], T. Fornal[6], G. Fuchert[1], O. Grulke[1], M. Hirsch[1], J. Knauer[1], M. Kubkowska[6], A. Langenberg[1], H. P. Laqua[1], M. Otte[1], N. Pablant[5], E. Pasch[1], K. Rahbarnia[1], T. Schröder[1], J. Svensson[1], U. Wenzel[1], G.A. Wurden[3], and the W7-X team

[1]*Max-Planck-Institut für Plasmaphysik, Greifswald, Germany*
[2]*Max-Planck-Institut für Plasmaphysik, Garching, Germany*
[3]*Los Alamos National Laboratory, Los Alamos, NM 87544, USA*
[4]*Laboratorio Nacional de Fusión – CIEMAT, 28040 Madrid, Spain*
[5]*Princeton Plasma Physics Laboratory, Princeton, New Jersey 08543, USA*
[6]*IFPiLM, Hery Street 23, 01-497 Warsaw, Poland*

Introduction The first experimental campaign of the stellarator Wendelstein 7-X (W7-X) [1] has been started with a limiter configuration comprising of five inboard carbon-limiters instead of the island divertor configurations to be used for later operation. The plasmas, both with He and H_2 as working gases, are obtained by electron cyclotron resonance heating (ECRH) with gradually increased total energy input into the machine in order to avoid possible thermal overload on the limiters. The maximum ECR-heating power is around 4 MW and the longest discharge duration reaches 6 s. Maximum core electron temperature T_e of ~10 keV, ion temperature T_i ~2.0 keV and central electron densities ~5.0×10^{19} m^{-3} have been achieved. The discharges are usually terminated in two ways: (1) thermal decay after termination of ECRH and (2) radiative collapse (RC) due to enhanced impurity radiation during the ECRH. It has been observed by High Efficiency XUV/VUV Overview Spectrometer (HEXOS) [2] and Pulse Height Analysis (PHA) [3] diagnostics, that the main intrinsic impurity species in the plasma are low- and medium-Z ones, like carbon, nitrogen and oxygen, up to elements like chlorine, sulfur, fluorine, copper and occasionally iron. Due to the spectral emission being dominated by C- and O- line radiation both species are assumed to contribute predominantly to the total plasma radiation as a first guess. The radiative power loss of the plasma is monitored by the bolometer diagnostic system [4], which comprises two cameras observing the total plasma cross-section from the horizontal and vertical direction, respectively. Based on the bolometer measurements, the total radiated power and the local radiation distribution have been estimated.

Experimental results For the estimation of the total radiative power loss P_{rad}, the signals of the horizontal bolometer camera (HBC) are used. The lines of sight (LoS) of these channels cover the triangular-shaped cross section of the plasma with a spatial resolution of 4-5 cm [4]. The time resolution of the system is around 5 ms. The signals are usually below 0.1 mW (for typical P_{ECRH} = 2 MW), and often exceeding 1.0 mW during RC. Using the pre-calculated geometric matrix of the LoS, taking into account the lengths of the individual LoS and their poloidal and toroidal extensions the radiated power in the viewed plasma slice is deduced. The total radiated power, P_{rad}, from the whole plasma volume is then obtained by linear extrapolation to the entire relevant torus volume. Toroidal variations were not considered here. This will be subject to additional bolometers planned at other toroidal positions as a next step. For the discharges already analysed, the radiative power loss fraction $f_{rad} = P_{rad}/P_{ECRH}$, is around 25-40% during stationary plasma phases. P_{rad} increases both with n_e and ECR-heating power, depending strongly on the electron temperature and impurity concentrations. The first plasmas during an experimental day, performed after the glow-discharge operation, showed always lower f_{rad} due to lower impurity contents, being consistent with the reduced VUV/EUV emission of oxygen and carbon measured by HEXOS system.

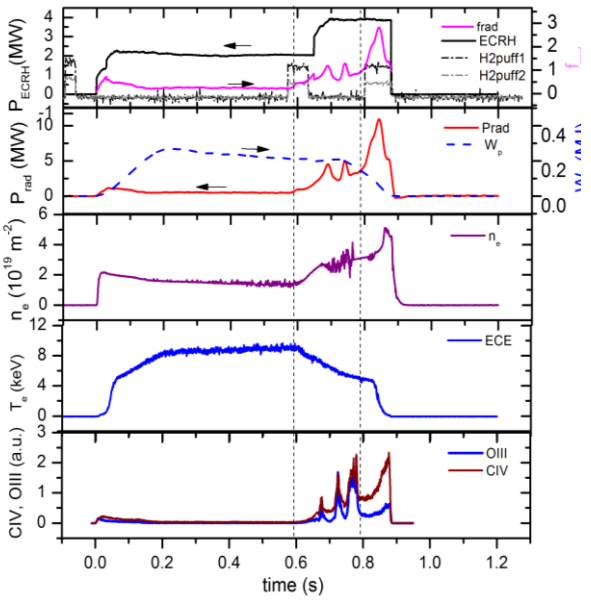

Fig. 1. Time traces of the RC-terminated discharge #20160309.007, a) absorbed ECR-heating power, radiative power loss factor and H_2-gaspuff timing, b) plasma stored energy and total radiated power loss, c) line-integrated density, (d) central electron temperature and (d) spectroscopy signals from OIII and CIV.

In the following part, we present the results of a RC-terminated H_2-plasma. In this discharge, Ar is prefilled as tracer gas for diagnostic purposes before the plasma pulse starts. The time traces of the discharge for selected parameters are shown in Fig. 1. When reaching the flat top phase (t ~ 0.2 s) following parameters have been reached: T_i measured by the X-ray imaging crystal spectrometer (XICS) [5] ~1.5 keV, the line-integrated electron density n_e measured by the interferometer ~1.5×10^{19} m^{-2} [6], the central T_e measured by ECE-diagnostic ~8 keV [7], the stored energy W_p obtained by diamagnetic loops ~220 kJ [8], and the radiative power loss P_{rad} ~500 kW with a loss factor f_{rad} ~ 25%.

Aiming at enhancing the plasma density, two additional H_2-gas puffs are applied at 0.57 s and 0.8 s and the heating power is increased to 4 MW shortly after the first one (see Fig.1). With the rise of n_e the O- and C-VUV line radiation as well as P_{rad} increases accordingly. The T_e drops first due to the increased cooling by impurity radiation and tends to recover slowly after the increase of P_{ECRH}. From the time point when P_{ECRH} is increased until the beginning of the RC, indicated by a rapid drop of W_p, the plasma exists in a transient phase, in which P_{rad} shows multiple excursions and f_{rad} is larger than 50% even reaching 100%. The C- and O-lines monitored by HEXOS show a similar behaviour as the bolometer signals, with slightly shifted peaking times. Detailed analysis for understanding this shift has been started.

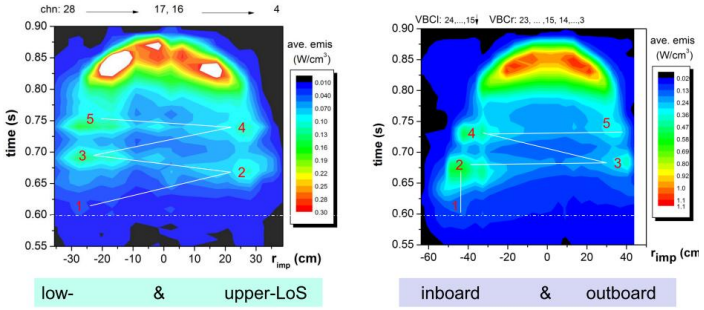

Fig. 2. Spatio-temporal evolutions of the chord-brightnesses measured by the horizontal (left) and the vertical (right) bolometer demonstrating the poloidally asymmetric emissivity pattern.

The oscillation-like signals of the impurity radiation motivate us to further investigate the local radiation distribution features. The tempo-spatial cord brightnesses of the two bolometers for the later time points (0.5-0.9 s) are displayed in Fig. 2, where r_{imp} stands for the impact radius of the LoS relative to the plasma center. The left picture shows 'hot-spots' which appear alternately in the upper- and lower plasma edge region; the right one demonstrates that these spots emit stronger at inboard side than at the outboard side. This poloidal asymmetric emissivity is clearly located in the outer region of the plasma ($\rho > 0.7$), where low-Z impurities such as C and O unambiguously contribute to the total radiation. The absolute contributions from other impurities will be analyzed after calibration of the HEXOS system. A tomographic reconstruction of the emissivity distribution based on Gaussian Process Tomography [11] has been carried out using the bolometer signals. The obtained 2D-emisivity profile for t = 0.75s is shown in Fig. 3, which demonstrates the poloiadally asymmetric emission distribution again.

The unstable impurity radiation intensity reflects an edge localized instability of the plasma parameters, which is also confirmed by T_e and n_e profile changes for t = 0.6s and 0.7s related to 0.5s, which are measured by Thomson scattering [9] (not shown here). This behavior might resemble MARFE-like properties observed in other machines [10]. The subsequent RC-phase begins shortly before 0.8 s, starting with further shrinking plasma dimensions and reduced radiation volume. The RC-phase is finally accellerated by the last

gas-puff: The plasma energy drops rapidly because P_{rad} significantly exceeds the net absorbed P_{ECRH} leading to plasma cooling.

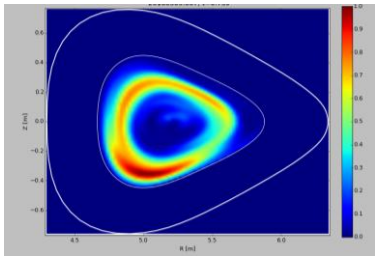

Fig. 3. A tomographic reconstruction of the 2D-emissivity distribution (t = 0.75s) showing the poloiadally asymmetric emission. The last closed flux surface (LCFS) is marked by the inner white line.

The possible mechanism for this edge localized oscillatoric instability is subject of ongoing investigations. Cross checks with other diagnostics, such as video [12] and IR-cameras monitoring the limiter tiles have been started [13]. The poloidally asymmetric emission patterns have also been detected by the video cameras showing toroidal non-axis-symmetric extension. The IR-camera demonstrates that in the transient phase plasma attachment to the limiter is unstable or partially, based on the reduction of the heat-load onto the limiter tiles compared to the flat top phase. Total detachment of the plasma to the limiter occurs in the later phase indicated by the drop of the limiter temperature. Further analysis to explain the observed thermal instability will be continued.

Acknowledgment

This work has been carried out within the framework of the EUROfusion Consortium and has received funding from the Euratom research and training programme 2014-2018 under grant agreement No 633053. The views and opinions expressed herein do not necessarily reflect those of the European Commission.

References:

1. H.S. Bosch et al., Nucl. Fusion 53, 126001 (2013)
2. B. Buttenschön, et al., this conference.
3. H. Thomsen, et al., J. Inst. 10, P10015 (2015)
4. D. Zhang, et al., Rev. Sci. Instrum. **81,** 10E134 (2010).
5. N. Pablant, et al. Europhysics Conference Abstracts 38F, P1.076 (2014).
6. J. Knauer, et al., this conference.
7. M. Hirsch, et al., this conference.
8. K. Rahbarnia, et al., this conference.
9. E. Pasch, et al, this conference
10. B. Lipschultz, et al., Nucl. Fusion. Vol.24, 977 (1984) ; H. Thomsen, et al., Nucl. Fusion 44, 820, (2004); B.J. Peterson, et al, J. Plasma Fusion Res. SERIES, Vol. 4, 432-436, (2001).
11. J. Svensson, JET Internal report, EFDA-JET-PR(11)24, (2011)
12. T. Szepesi, et al., this conference.
13. G. A. Wurden, et al., Rev. Sci. Instrum. 2016; 21st HTPD 2016, Madison, Wisconsin, USA.